

Mechanical performance of heavy gauge press hardened steel modified with Nb and Mo additions on GMAW welded joints

Tiago Führ¹Diego Tolotti¹Daniela Bertol^{1*} João Henrique Corrêa de Souza¹Angélica Paola de Oliveira Lopes¹

Abstract

The principle of hot stamping is directly related to the opportunities offered by the chemical composition of boron-alloyed steel due to the process amplitude window for quenching. The 22MnB5 + NbMo steel presents a microstructure composed of ferrite-perlite with yield limit and resistance limit of approximately 450 and 600 MPa, respectively. After the workpiece is hot stamped, the microstructure obtained is completely martensitic, and can reach strength limit values exceeding 1500 MPa. This paper presents a study on the 22MnB5 weldability, mechanical and microstructural properties when designed with Nb and Mo additions, hot formed, and welded using three different wires (AWS A5.28 ER110S-G, E110C-G M H4 and ER70S-6), evaluating these properties through metallographic and macrographic analysis, tensile tests and Charpy impact fractography. According to the results, it is possible to weld 22MnB5 + NbMo press hardened steels, with best condition obtained in this work using ER110S-G wire, considering fracture toughness and satisfactory tensile test results.

Keywords: Presshardening steel; Hot stamping; Welding metallurgy; Alloy design.

Desempenho mecânico de aço endurecido de prensa de medidor pesado modificado com adições de Nb e Mo em juntas soldadas de GMAW

Resumo

O princípio da estampagem a quente está diretamente relacionado às oportunidades oferecidas pela composição química do aço ligado a boro devido à amplitude da janela no processo de têmpera. O aço 22MnB5 + NbMo apresenta uma microestrutura composta por ferrita-perlita com limite de escoamento e limite de resistência de aproximadamente 450 e 600 MPa, respectivamente. Após a peça estar estampada a quente, a microestrutura obtida é completamente martensítica, podendo atingir valores limite de resistência superiores a 1500 MPa. Este trabalho apresenta um estudo sobre a soldabilidade, propriedades mecânicas e microestruturais do aço 22MnB5 quando refinado com adições de Nb e Mo, conformado a quente e soldado utilizando três diferentes arames classificados pela norma AWS A5.28 (ER110S-G, E110C-G M H4 e ER70S-6), avaliando essas propriedades por meio de análise metalográfica e macrográfica, ensaios de tração e fractografia de impacto Charpy. Os resultados mostram que é possível soldar o aço 22MnB5 + NbMo temperado com sucesso, sendo a melhor condição obtida neste trabalho ao usar o arame ER110S-G, considerando tanto a tenacidade à fratura quanto os resultados satisfatórios nos ensaios de tração.

Palavras-chave: PHS; Estampagem a quente; Metalurgia de solda; Design de liga.

1 Introduction

The increasing effort of the automobile industry in the search of mass reduction and the increase of vehicles safety demands the use of structural components made with

higher mechanical resistance steels. On the other hand, the continuous effort to increase productivity and reduce manufacturing costs requires structural steels for hot stamping,

¹Bruning Tecnometal Ltda., Panambi, RS, Brasil.

*Corresponding author: bertodaniela@gmail.com; daniela.bertol@bruning.com.br



since this process allows producing structural components with complex geometries and free of elastic return after the stamping. In this context, as presented by Hein [1], 22MnB5 press hardening steel (PHS) was developed with the aim of improving the structural parts and high strength reinforcements production and performance by the use of hot stamping technology. Mohrbacher [2] proved that, when using 22MnB5 steels with thickness higher than 3mm, some metallurgical refinement can be made by adding Nb and Mo to this alloy, improving its quenching capability and weldability. These alloying metals in PHS also guarantee better austenite grain size control, improved low temperature toughness and better critical bending angle, as studied by Zhang et al. [3]. Bian et al. [4] discovered that Nb microalloying can reduce sensitivity to hydrogen embrittlement-induced cracks due to hydrogen trapping and grain refinement, and, by adding 0.05 w.% Nb, critical fracture stress can also be increased more than double.

In addition, the joining of hot-stamped parts can be done by resistance spot welding, laser welding and GMAW welding. However, there is not much information in the literature on the weldability characteristics of these steels using the Gas Metal Arc Welding (GMAW) welding process, especially when sheets with thicknesses over 3 mm are required. Thus, the present work evaluated the 22MnB5 steel, modified with Nb and Mo additions, weldability of thick plates after hot stamping in top joint, having as parameter the mechanical behavior of welded joints. Three different

welding wires were tested (ER110S-G, E110C-G M H4 and ER70S-6 considering AWS A5.28 standard), using previously validated welding parameters, in order to define the best condition to evaluate the PHS alloy joining.

2 Experimental procedure

2.1 Sample preparation and characterization

Steel plates of 7 mm thickness were cut with a Bysprint Fiber 3015 Bystronic laser cutting machine as presented in Figure 1a. Several evaluations and tests were carried out to study the main variables involved in the welding process of 22MnB5 with Nb+Mo material. The main characterization analysis were through metallography and weld macroscopic analysis, tensile test, and Charpy impact fractography. The specimens were removed by wire electro-discharge cutting and the regions were cut according to DIN EN ISO 15614-1: 201. Chemical composition of the 22MnB5 steel with and without Nb+Mo additions were analyzed by atomic emission spectrometry, and results are shown in Table 1.

2.2 Hot forming

The first step of hot stamping process consists in the blank austenitization in a furnace. In the industrial process, the blank is heated in the range between 850 and 950 °C and

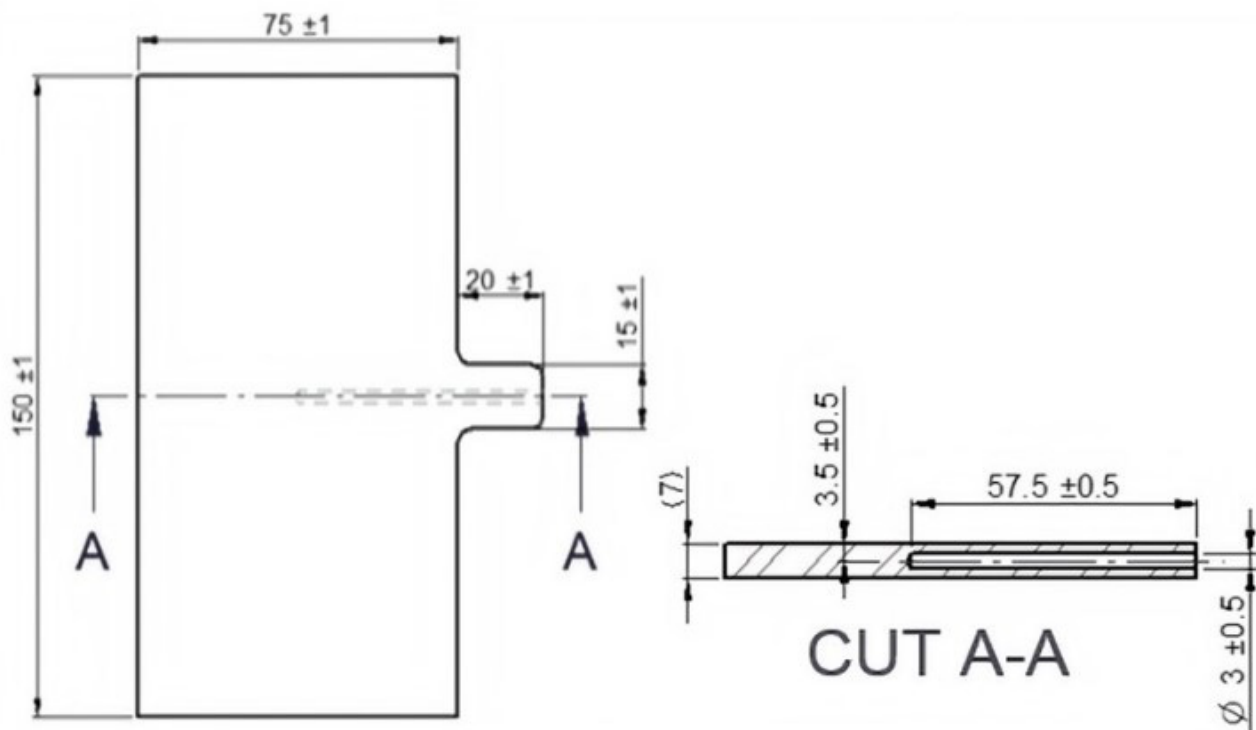


Figure 1. Laser cut samples dimensions.

then transferred to the press in fully austenitic conditions. The use of cooled dies assures a rapid cooling of the sheet in order to obtain a martensitic microstructure, since the temperature of martensite start was found to be 382°C, according to Turetta et al. [5]. In addition, Souza et al. [6] observed that austenitization times in furnace can vary from 5 to 10 minutes without affecting final microstructure, once the blank temperature is raised to approximately 950 °C transferred quickly from the austenitizing furnace to the press. In order to avoid bainitic formation and to obtain a 100% martensitic microstructure, which is expected from the hot stamping process, the cooling rate should be at least 27 °C/sec, as observed by Karbasian and Tekkaya [7]. The coolant used during the hot stamping process in this study was water and the process parameters are presented in Table 2. After the presshardening process, the specimens were covered with a thin layer of mill scale. In that case, a brushing process before the weld was performed, in order to reduce the instability of the electric arc, avoiding problems like porosity in the welded cord.

2.3 Welding

In order to define the GMAW welding parameters, preliminary tests were taken by varying the welding current values of these samples. Welding tests were carried out with welding current of 270 A and voltage of 25,2 V. Three different wires were tested:

- **Weld condition 1** – solid wire, with 1,2 mm diameter, whose classification defined by the AWS Standard A5.28 is ER110S-G;
- **Weld condition 2** – low carbon solid wire, whose classification defined by the AWS Standard A5.28 is ER70S-6;
- **Weld condition 3** – metal cored wire, whose classification defined by the AWS Standard A5.28 is E110C-G M H4.

Welding velocity was 380 mm/min, with wire velocity of 11,6 m/min and weld joint gap of 3 mm. The protective

gas used was 10% CO₂ + 90% Ar, with flow of 15 L/min. For all welding conditions, a copper backing was used according to the joint design specified in ISO 9692-1: 2003.

3 Results and discussion

3.1 Microstructural characterization

The 22MnB5+NbMo microstructural analysis before and after hot forming process are show in Figures 2a, b, respectively.

Through this analysis it was possible to notice that the microstructure of 22MnB5 + Nb+Mo in its initial condition is composed of a mixture of ferrite and perlite, while the base material after hot stamping revealed a refined microstructure entirely martensitic. After the welding tests, the microstructural analysis of the heat affected zone (HAZ) and the limit region between weld metal and HAZ are presented in Figures 3-5.

It is possible to note, for all conditions, that a bainitic microstructure was also formed at the HAZ. In the transition zone, between the molten zone and the HAZ, the precipitation of carbides in grain boundary was observed, as well as a refined microstructure composed of Widmanstätten ferrite, as well as bainite.

3.2 Welded joints macrographic analysis

By means of macrographic analysis, it was possible to analyze the quality of the welded joints, being verified that all samples had total weld penetration. No discontinuities such as pores, cracks, inclusions of slag and lack of fusion were found in any of the analyzed samples. Figure 6 shows the macrography regarding weld conditions, where it is possible to identify the formation lines of the HAZ and the weld metal. Figure 6a shows that penetration was complete for all conditions, where condition 1 presented the best weld reinforcement measured, for both face (DL2) and weld root (DL3) reinforcements.

Table 1. Chemical composition comparison between 22MnB5 alloy and with Nb+Mo additions

Material	Chemical composition (Weight %)									
	C	Si	Mn	Cr	Ni	Mo	Ti	Nb	Al	B
22 MnB5	0,22	0,23	1,24	0,2	0,01	0,01	0,048	0,003	0,04	0,003
22MnB5+Nb+Mo	0,22	0,17	1,17	0,25	<0,1	0,16	0,03	0,047	0,014	0,002

Table 2. Presshardening parameters

Soaking temperature (°C)	Soaking time (min)	Water flow in the cooling channels (L/min)	Contact pressure (MPa)	Press force (Ton.)	Cooling channels temperature (°C)	Transfer time to press (s)
950	5	13	70	80	5	< 7

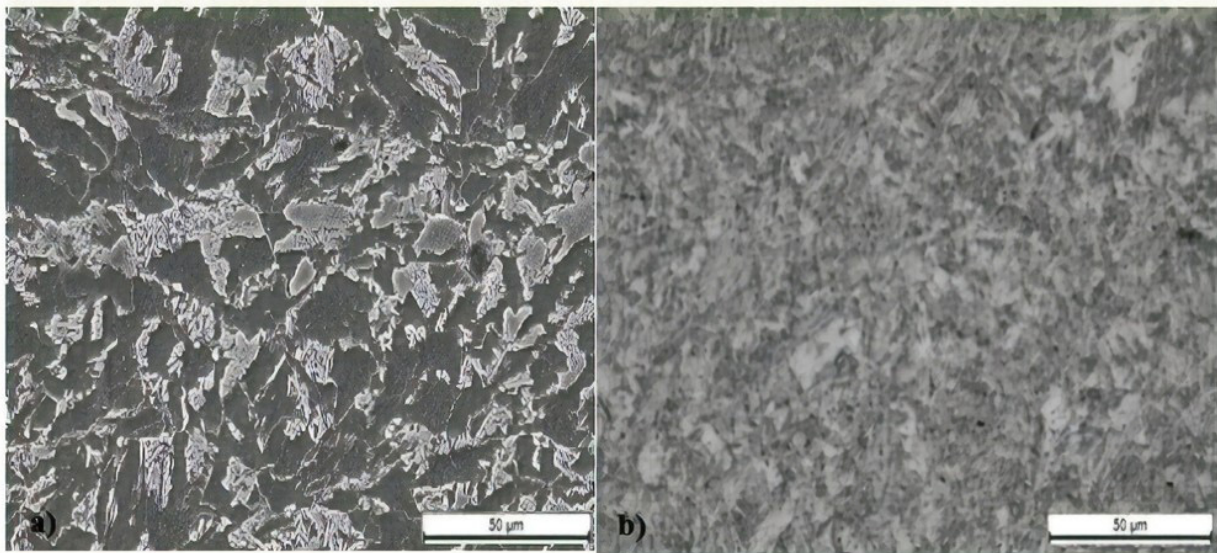


Figure 2. Microstructure of 22MnB5 + Nb+Mo steel before presshardening (a) with the presence of ferrite and perlite, and after presshardening (b), completely martensitic (5000x).

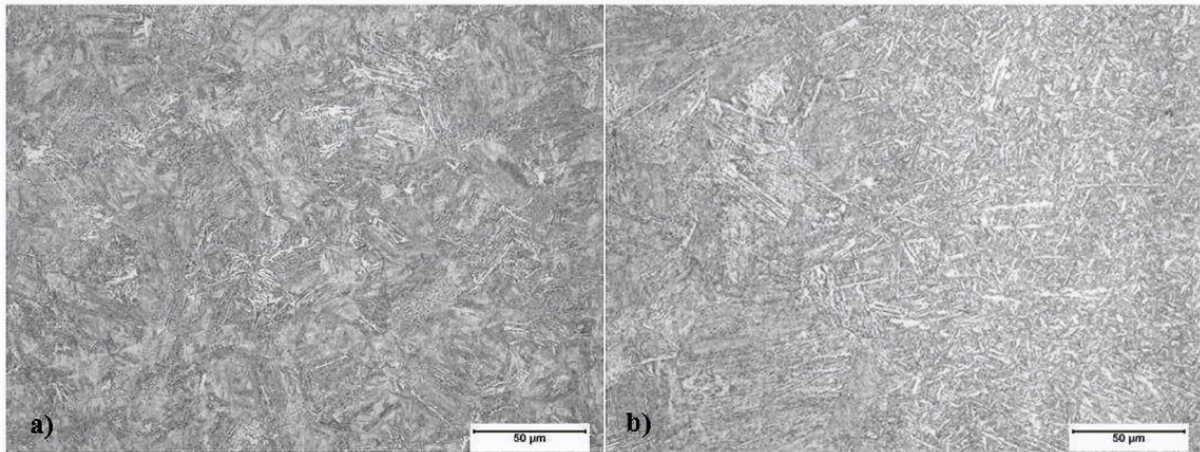


Figure 3. Micrograph showing the microstructure of HAZ for condition 1 (a) and at the boundary between the weld metal and the HAZ for condition 1 (b).

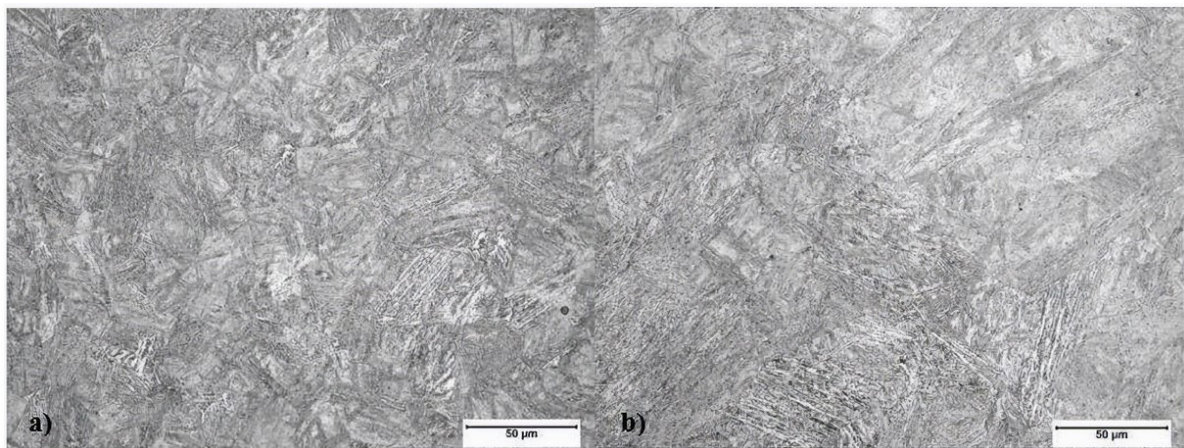


Figure 4. Micrograph showing the microstructure of HAZ for condition 2 (a) and at the boundary between the weld metal and the HAZ for condition 2 (b).

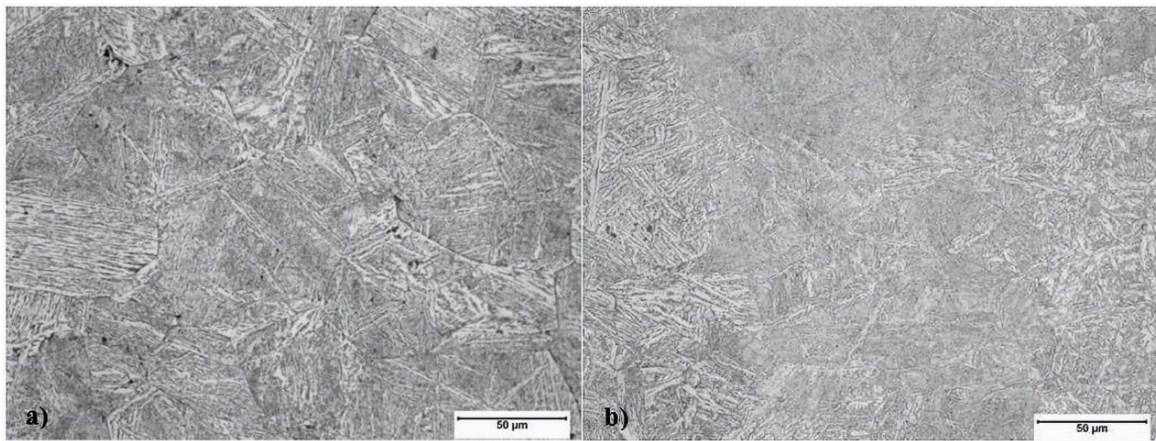


Figure 5. Micrograph showing the microstructure of HAZ for condition 3 (a) and at the boundary between the weld metal and the HAZ for condition 3 (b).

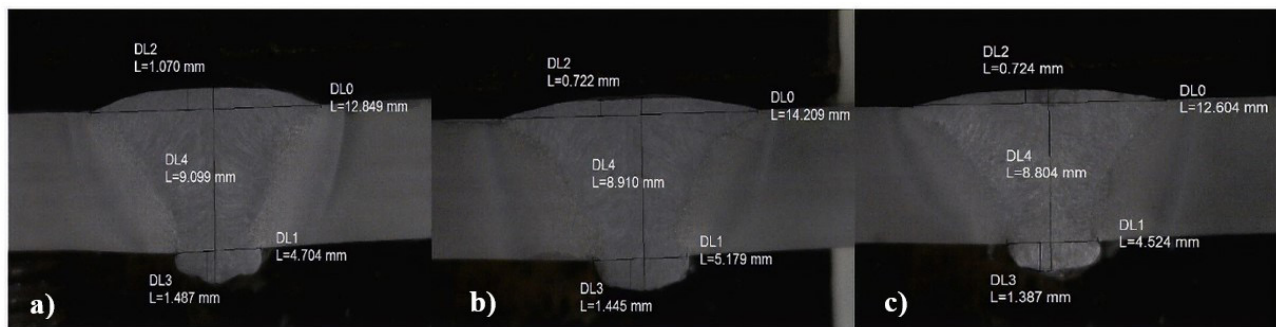


Figure 6. Macrography of (a) weld condition 1; (b) weld condition 2; and (c) weld condition 3.

3.3 Tensile tests

Tensile tests were carried out to evaluate the maximum tensile stress, tensile yield stress and elongation for all welding conditions, in order to evaluate the mechanical behavior of welds and to verify the best welding wire for this steel. Obtained values from PHS tensile tests before and after the presshardening process are presented in Table 3.

After the presshardening step, the samples were welded according to weld conditions described previously, and the tensile test results using different welding wires are presented in Table 4.

As shown in Table 4, the welding condition 3, with the cored metal wire E110C-G M H4, presented a higher resistance limit when compared to the other two types of solid wire. However, ER110S-G presented a good intermediary condition, with slightly less resistance but higher total elongation.

3.4 Charpy impact fractography

The impact tests were carried out to evaluate the impact strength of the weld of all the study conditions at different application temperatures in order to evaluate the behavior of the addition materials and verify the best welding condition.

Table 3. Tensile test results before and after the presshardening process

Before presshardening			
Sample	Max. Stress (MPa)	Yield Stress (MPa)	Total Elongation (%)
1	769	636	20,18
2	770	651	21,12
3	787	639	16,88
Mean	775	642	19,39
Dev.	8,26	6,48	1,82
After presshardening			
Sample	Max. Stress (MPa)	Yield Stress (MPa)	Total Elongation (%)
1	1453	1075	9,98
2	1475	1077	10,52
3	1467	1073	10,28
Mean	1465	1075	10,26
Dev.	9,09	1,63	0,22

Table 4. Tensile test results after welding process

Welding condition	Max. Stress (MPa)	Yield Stress (MPa)	Total Elongation (%)
(1) ER110S-G	968	779	8,66
(2) ER70S-6	827	699	9,18
(3) E110C-G M H4	1060	913	7,81

The results of the weld material on impact toughness tests on the studied conditions are plotted in the graph of Figure 7.

As shown in Figure. 7, for welding conditions 1, 2 and 3, the ER70S-6 welding wire presented the highest impact toughness results; there was a higher energy absorption for all temperatures tested, in addition to presenting a homogeneity of the results. In contrast, the metal-cored wire E110C-G M H4 showed the lowest impact toughness results, with lower energy absorption for all tested temperatures. The ductile-brittle transition curve is related to the dependence of the energy absorbed by the Charpy test sample in relation

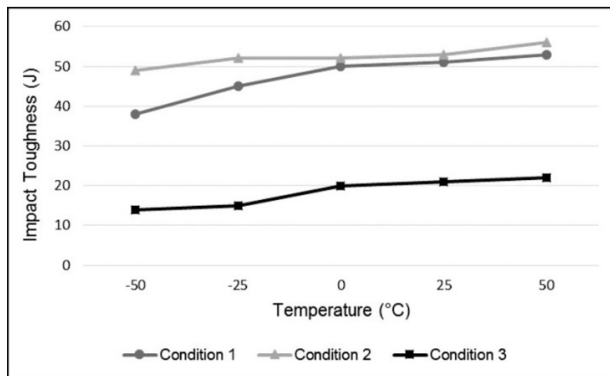


Figure 7. Impact toughness results for conditions 1, 2 and 3.

to temperature. Normally, as observed by Silva et al. [8], the curve has an upper plateau, where the fracture occurs ductile, and a lower plateau, characterized by a fragile fracture. Additionally, the curves has a transition region in which the ductile and fragile fracture modes compete, with both cleavage and ductile tearing failures coexisting. For the studied conditions, all the materials presented a perceptible ductile-fragile transition, with curves similar to other materials with martensitic microstructure, as shown by Zhao et al. [9].

Figures 8a, b corresponds to condition 1 sample fracture at test temperature of 25°C and Figures 8c, d at -50°C. The high amount of spherical dimples present in the region of fracture origin (Figure 8b) indicates a ductile fracture mechanism, a result that matches the values of energy absorbed in the test. Contrarily, the high amount of cleavage facets present in the region of fracture origin (Figure 8d) indicates a fragile fracture mechanism.

Moreover, Figures 9 and 10 also represents the sample fracture at both test temperatures for conditions 2 and 3, respectively. At test temperature of 25°C, it is observed for weld condition 2 sample the same behavior as condition 1 sample, in contrast of condition 3 sample, which presented a fracture with cleavage facets and regions with dimples formation, characteristic of fracture mode called mixed. The presence of micro pores in the lower part can be possibly due to a lack of gas protection or low gas flow.

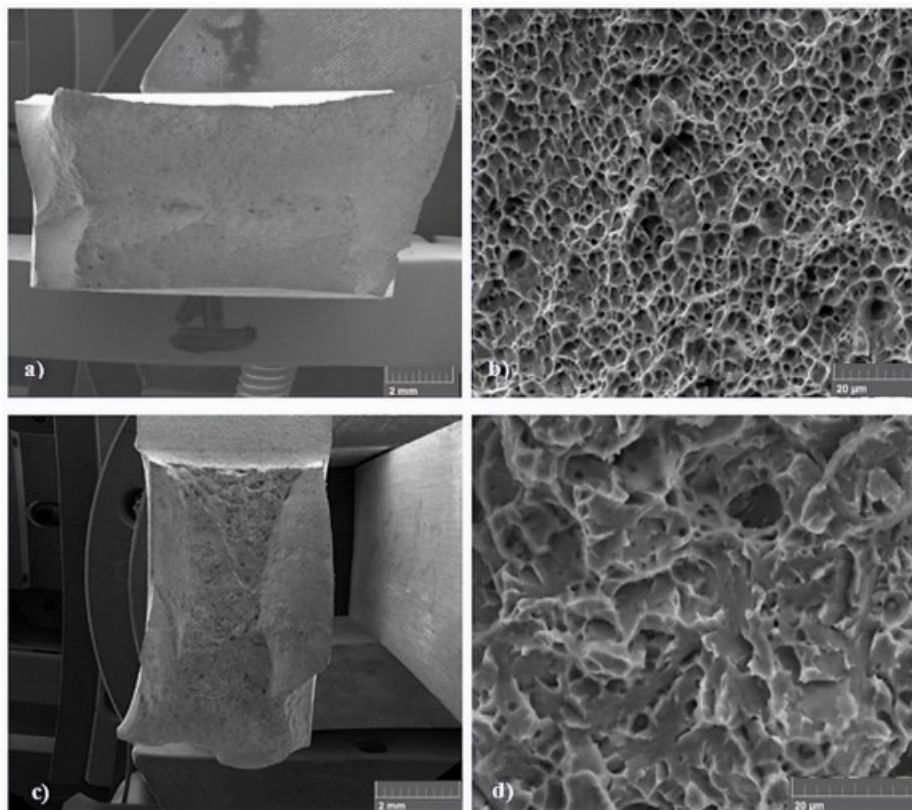


Figure 8. Charpy fractography analysis for condition 1 (a) at 25°C with 30x magnification; (b) 4000x magnification; (c) at -50°C with 40x magnification; and (d) 6000x magnification.

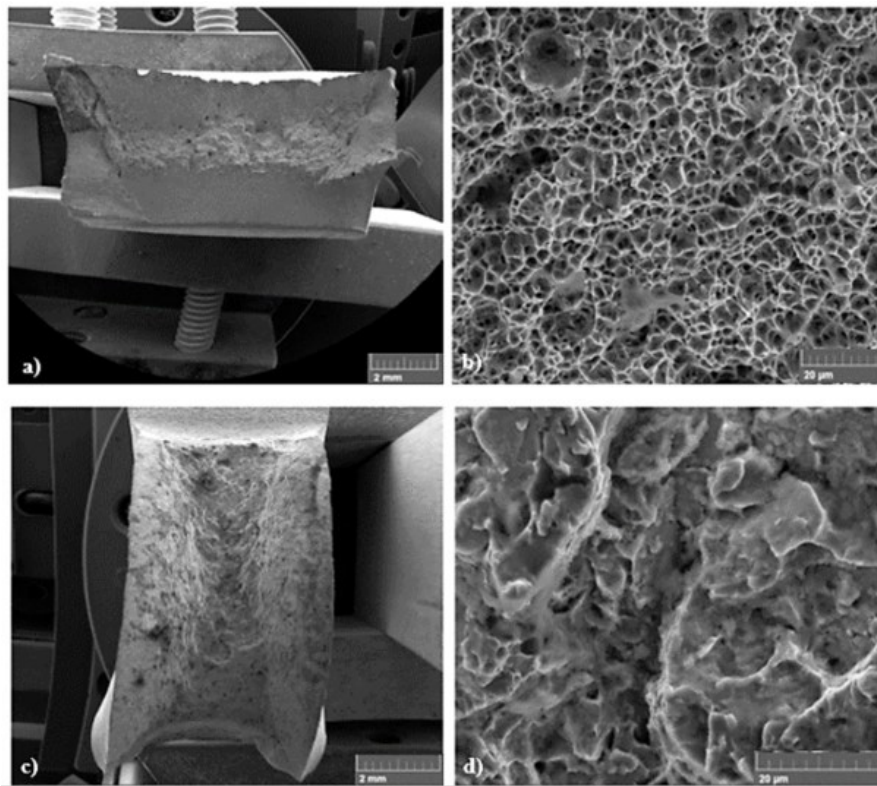


Figure 9. Charpy fractography analysis for condition 2 (a) at 25°C with 30x magnification; (b) 4000x magnification; (c) at -50°C with 40x magnification; and (d) 6000x magnification.

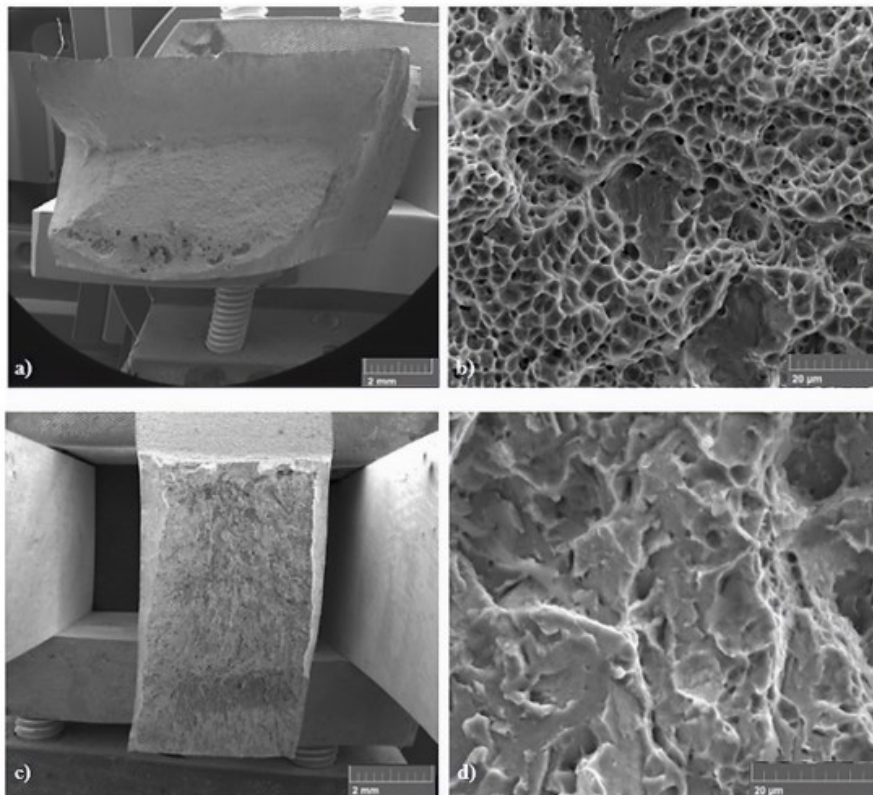


Figure 10. Charpy fractography analysis for condition 3 (a) at 25°C with 30x magnification; (b) 4000x magnification; (c) at -50°C with 40x magnification; and (d) 6000x magnification.

For test temperature of -50°C , it is possible to observe the same fracture mechanism for all weld conditions. Considering findings presented by Lin et al. [10], in which the fractography of Nb-free specimen exhibits typical brittle intergranular fracture, it can be confirmed that Nb microalloying increases ductile dimple-type fracture pattern, causing an enhancement of intergranular strength.

4 Conclusions

The metallographic analysis confirmed that the hot forming was successful, since martensitic microstructure was obtained homogeneously throughout the samples. The tensile strength of 22MnB5 + NbMo steel showed a significant increase from an average of 775 MPa to 1465 MPa. Additionally, it was verified that the base material of all the samples presented a refined microstructure and composed of tempered martensite. In the thermally affected zones, a bainitic microstructure was generated and in the transition

zone, between the molten zone and the thermally affected zone, the precipitation of carbides in grain boundary was observed. Most samples of the weld metal presented a refined microstructure composed of acicular ferrite, polygonal ferrite and Widmanstätten ferrite, as well as carbide aggregates.

At the end of this study, it is concluded that the condition 1 showed the best results, being the most suitable for use in the manufacture of welded components with 22MnB5 + NbMo steel, followed by condition 2. Although condition 3 showed higher mechanical tensile strength, it presented unsatisfactory results in Charpy impact tests.

Acknowledgements

Research presented in this paper was only made possible by the firm partnership between Bruning Tecnometal Ltda, CBMM, Niobelcon BVBA and SSAB Europe. The authors gratefully acknowledge these partners.

References

- 1 Hein P. A global approach of the finite element simulation of hot stamping. *Advanced Materials Research*. 2005;6-8:763-770. <http://dx.doi.org/10.4028/www.scientific.net/AMR.6-8.763>.
- 2 Mohrbacher H. Property optimization in as-quenched martensitic steel by molybdenum and niobium alloying. *Metals*. 2018;8(4):234. <http://dx.doi.org/10.3390/met8040234>.
- 3 Zhang S, Huang Y, Sun B, Liao Q, Lu H, Jian B, et al. Effect of Nb on hydrogen-induced delayed fracture in high strength hot stamping steels. *Materials Science and Engineering: A*. 2015;626:136-143. <http://dx.doi.org/10.1016/j.msea.2014.12.051>.
- 4 Bian J, Mohrbacher H, Zhan S, Lu H, Wang W, Zhang Y, et al. Impact of Nb Microalloying on the Hydrogen Embrittlement of Press Hardening Steel. In: *Proceedings of 5th International Conference on Hot Sheet Metal Forming of High Performance Steel*; 2015 May 31-June 3; Toronto, Canada. Toronto: Verlag Wissenschaftliche Scripten; 2015. p. 65-74.
- 5 Turetta A, Bruschi S, Ghiotti A. Investigation of 22MnB5 formability in hot stamping operations. *Journal of Materials Processing Technology*. 2006;177:396-400. <http://dx.doi.org/10.1016/j.jmatprotec.2006.04.041>.
- 6 Souza JHC, Almeida DT, Mohrbacher H, Suikkanen P. Development of process techniques for press hardening of thick plates. In: *New Developments in Sheet Metal Forming Conference*; 2018 May 9th-10th; Stuttgart, Germany. Stuttgart: MAT INFO Werkstoff- Informationsgesellschaft; 2018.
- 7 Karbasian H, Tekkaya AE. A review on hot stamping. *Journal of Materials Processing Technology*. 2010;210:2103-2118. <http://dx.doi.org/10.1016/j.jmatprotec.2010.07.019>.
- 8 Silva CA, Nascimento RCR, Martins MS, Freitas MCS. Influence of temperature on ductile-fragile behavior. *Materials Science Forum*. 2014;802:383-387. <http://dx.doi.org/10.4028/www.scientific.net/MSF.802.383>.
- 9 Zhao YJ, Su YM, Liu M, Hu ZL, Tang P. Ductile-to-brittle transition and impact fracture behavior of 3Mn-Si-Ni low carbon martensitic steel. *Strength of Materials*. 2019;51:291-299. <http://dx.doi.org/10.1007/s11223-019-00075-8>.
- 10 Lin L, Li B, Zhu G, Kang Y, Liu R. Effect of niobium precipitation behavior on microstructure and hydrogen induced cracking of press hardening steel 22MnB5. *Materials Science and Engineering: A*. 2018;721:38-46. <http://dx.doi.org/10.1016/j.msea.2018.02.021>.

Received: 10 June 2019

Accepted: 19 July 2021